Lifetime measurement after direct transfer reactions with AGATA at LNL

Franco Galtarossa[1,*], *Andrea* Gottardo[2], *Luca* Zago[2,3], *Matúš* Balogh[2], *Elia* Pilotto[1,3], *Giorgia* Pasqualato[4], *Daniele* Mengoni[1,3], *Pablo* Aguilera Jorquera[1], *Giuseppe* Andreetta[2,3], *Filippo* Angelini[2,3], *Lucia* Baldesi[5], *Jaime* Benito[1], *Giovanna* Benzoni[6], *Simone* Bottoni[6,7], *Daniele* Brugnara[2], *Alberto* Camaiani[5], *Sara* Carollo[1,3], *Javier* Collado[2], *Giacomo* Corbari[5,6], *Maurizio* D'Andrea[8], *Giacomo* De Angelis[2], *Mirco* Del Fabbro[2,9], *Daniele* Dell'Aquila[10,11], *Josipa* Diklić[12], *Felix* Dunkel[13], *Federica* Ercolano[10,11], *Aysegul* Ertoprak[2], *Andres* Gadea[14], *Agnese* Giaz[6], *Alain* Goasduff[2], *Benito* Góngora-Servín[2,9], *Andrea* Gozzelino[2], *Kasia* Hadyńska-Klek[15], *Corentin* Hiver[4], *Zhen* Huang[1], *Massyl* Kaci[4], *Hannah* Kleis[13], *Silvia Monica* Lenzi[1,3], *Ivano* Lombardo[16], *Naomi* Marchini[5], *Hannes* Mayr[17], *Roberto* Menegazzo[1], *Nicolas* Miani[3], *Adriana* Nannini[5], *Daniel Ricardo* Napoli[2], *Raquel* Nicolás del Álamo[1,3], *Julgen* Pellumaj[2,9], *Rosa Maria* Pérez-Vidal[2], *Sara* Pigliapoco[1,3], *Marta* Polettini[1], *Francesco* Recchia[1,3], *Luigi* Redigolo[16], *Kseniia* Rezynkina[1], *Marco* Rocchini[5], *Matúš* Sedlák[2,18], *Andrej* Spacek[15], *Franziskus* Spee[13], *Giulia* Spina[7], *Damiano* Stramaccioni[2,3], *José Javier* Valiente-Dobón[2], *Irene* Zanon[2], and *Guangxin* Zhang[1]

[1]Istituto Nazionale di Fisica Nucleare, Sezione di Padova, Padova, Italy
[2]Istituto Nazionale di Fisica Nucleare, Laboratori Nazionali di Legnaro, Legnaro (PD), Italy
[3]Dipartimento di Fisica e Astronomia, Università degli Studi di Padova, Padova, Italy
[4]IJCLab, IN2P3/CNRS, Université Paris-Saclay, Orsay, France
[5]Istituto Nazionale di Fisica Nucleare, Sezione di Firenze, Firenze, Italy
[6]Istituto Nazionale di Fisica Nucleare, Sezione di Milano, Milano, Italy
[7]Dipartimento di Fisica, Università degli Studi di Milano, Milano, Italy
[8]Istituto Nazionale di Fisica Nucleare, Laboratori Nazionali del Sud, Catania, Italy
[9]Dipartimento di Fisica e Scienze della Terra, Università di Ferrara, Ferrara, Italy
[10]Dipartimento di Fisica "Ettore Pancini", Università degli Studi di Napoli "Federico II", Napoli, Italy
[11]Istituto Nazionale di Fisica Nucleare, Sezione di Napoli, Napoli, Italy
[12]Ruđer Bošković Institute, Zagreb, Croatia.
[13]Institute für Kernphysik, University of Cologne, Cologne, Germany
[14]Instituto de Física Corpuscular, CSIC-Universidad de Valencia, E-46980 Valencia, Spain
[15]HIL, University of Warsaw, Warsaw, Poland
[16]Università di Catania and INFN Sezione di Catania, Catania, Italia
[17]Technische Universität Darmstadt, Institut für Kernphysik, Darmstadt, Germany
[18]Institute of Physics, Slovak Academy of Sciences, Bratislava, Slovakia

Abstract. Lifetimes of nuclear excited states are important observables in nuclear structure studies, since they can directly be related to electromagnetic transition matrix elements. The determination of transition probabilities between nuclear states provides information on their microscopic structure and represents an important benchmark for nuclear structure models. In recent experiments at INFN Legnaro National Laboratories, we coupled the newly installed γ-ray tracking spectrometer AGATA with light charged-particle detection systems to perform lifetime measurements after one- and two-nucleon direct transfer reactions at 5-10 AMeV. In this contribution, we will present two cases, related to the measurement of lifetimes in the femtosecond and picosecond range in ^{37}S and ^{56}Ni, on the basis of which the possibilities offered by this kind of set-up and some preliminary results will be discussed.

1 Introduction

The AGATA γ-ray tracking array [1] has been installed at the INFN Legnaro National Laboratories (LNL) in 2021 and started its first physics campaign in May 2022. In the current installation, AGATA is coupled to the large-acceptance magnetic spectrometer PRISMA [2, 3]. Thanks to the excellent resolutions in mass A and charge Z for heavy ions ($30 \lesssim A \lesssim 140$) offered by the magnetic spectrometer, this coupling allows to perform γ-ray spectroscopy and lifetime measurement of nuclear excited states after Multi-Nucleon Transfer (MNT) at energies close to the Coulomb barrier or fusion-fission reactions. Besides PRISMA, AGATA can be coupled to a series of other ancillary detectors, such as Silicon arrays, MCP detectors and scintillators [4]. This makes the set-up extremely versatile and expands significantly the types of reactions that can be studied. Fusion-evaporation, Coulomb excitation, proton inelastic scattering and direct transfer

*e-mail: franco.galtarossa@pd.infn.it

reactions are some examples.

Direct transfer reactions, in which one or two nucleons are exchanged between projectile and target, have been largely studied since the early days of Nuclear Physics thanks to their preference to populate states of single-particle nature and their high sensitivity to the transferred angular momentum, which allowed the determination of spin and parity of ground and excited states in the final nucleus. In some specific cases, these characteristics can make them the reactions of choice also for lifetime measurements of nuclear excited states. Coupling light charged-particle detectors with γ-ray detector arrays, one can achieve high suppression of the background and large control on feeding transitions thanks to the unmatched Q-value resolution attainable with these reactions [5]. In addition, their selectivity allows the study of states that are not easily accessible with other types of reactions. In particular, Coulomb excitation is ideal to study collective yrast states; multi-nucleon transfer (MNT) reactions populate mainly yrast states with medium-to-high spin and only little transfer strength goes to non-yrast states [6]; fusion-evaporation and fission reactions generally populate higher-spin states but, since the nucleus is populated at high excitation energies and it is difficult, in these reactions, to have full control on the reaction Q value, the effect of the possible presence of long-lived feeding transitions on the lifetime determination may be hard to assess; finally, inelastic scattering reactions allow for the population of both yrast and non-yrast states, but the study of exotic nuclei with such reactions requires the use of exotic beams. Therefore, direct transfer reactions represent one of the best, and in some cases unique, tools to perform γ-ray spectroscopy and lifetime measurement of selected non-yrast states in unstable nuclei.

In this contribution we will focus on only two of the many cases recently studied with AGATA at LNL, where lifetimes of nuclear excited states were measured after one- and two-nucleon transfer reactions. In particular, in Section 2 we will present a (d, p) reaction in inverse kinematics to measure lifetimes of intruder states in ^{37}S, while in Section 3 a lifetime measurement in the doubly-magic ^{56}Ni nucleus via a two-proton transfer reaction with heavy ions will be discussed. Although the analysis of these experiments is ongoing, the possibilities offered by the coupling of AGATA with different charged-particle detectors in terms of selection and resolving power can already be appreciated.

2 Lifetime measurements of intruder states in ^{37}S

The island of inversion (IoI) at $N = 20$ around ^{32}Mg is one of the most famous examples of a quadrupole-deformed intruder configuration becoming the ground state, thereby effectively making the $N = 20$ shell closure disappear. It has been successfully described by shell-model calculations as the mixing of neutron $np-nh$ configurations (with n up to 8). These calculations indicate that the $(sd)^{-n}(fp)^n$ intruder configurations, at several MeV in the $Z = 20$ ^{40}Ca nucleus, gradually lowers in energy with decreasing Z, as an effect of increasing quadrupole correlations in combination with a decrease of the $d_{3/2} - f_{7/2}$ $N = 20$ gap [7]. In this regard, the odd-even isotones at $N = 21$ have been studied extensively, because the appearance of intruder states can be readily compared to single-particle states in the fp shells, $1p$ states in the following, helping to understand the mixing of intruder and normal configurations [8, 9].

In $N = 21$ isotones, positive-parity ($1/2^+$ and $3/2^+$) intruder states have $1h - 2p$ nature, while negative-parity ($3/2^-$ and $7/2^-$) intruder states have instead $2h - 3p$ as dominant configuration. In ^{39}Ar ($Z = 18$), the $3/2^+$ and $1/2^+$ states are found at energies of 1.5 MeV and 2.4 MeV, respectively, while the $2h - 3p$ $3/2^-$ and $7/2^-$ intruder states are found at around 2.5 MeV. In ^{37}S ($Z = 16$), such intruder configurations appear at lower energy, as expected approaching the island of inversion. In this nucleus a strong E2 branching is observed from the intruder ($7/2^-$) at 2023 keV towards the *a priori* $1p$ $3/2^-$ state at 646 keV, which takes a large fraction of the $p_{3/2}$ single-particle strength [10]. Such branching is absent in ^{39}Ar and one may wonder whether its appearance in ^{37}S is due to an unexpectedly large mixing between normal and intruder configurations already at $Z = 16$, so quite far from the center of the IoI. Shell model calculations with the *sdpf-u-mix* interaction are in fact unable to reproduce such branching.

The determination of the degree of mixing between spherical and deformed intruder configurations can be obtained measuring electromagnetic transition probabilities, in particular electric quadrupole (E2) transitions which are particularly sensitive to collectivity, between intruder and spherical states. In the case of ^{37}S, the states of main interest are the $1h - 2p$ $3/2^+$ state at 1397 keV and the $2h - 3p$ states $3/2^-$ at 1992 keV and $7/2^-$ at 2023 keV. The lifetimes of these states are expected to lie in very different ranges: the $3/2^+$ state, which decays to the 646-keV state via an E1 transition of 751 keV, should lie in 10-100 ps range, while the $3/2^-$ and the $7/2^-$ states, where E2 and M1 transitions are competing, are instead in the 50-500 fs range.

Lifetimes in the ps range are usually measured by means of the Recoil Distance Doppler Shift (RDDS) technique, placing a stopper or a degrader at a given and changeable distance d from the target. Computing the number of ions emitted in flight between target and stopper and at rest in the stopper (or after the degrader), as a function of d, the level lifetime can be determined. Lifetimes in the fs region are instead measured via the Doppler Shift Attenuation Method (DSAM), where target and degrader (or stopper) are stick together and one looks at the line shape of the γ-ray transition of interest. The two techniques are described in Ref. [11]. In the experiment here presented, they were combined in a single measurement.

We employed the neutron adding reaction ^{36}S$(d, p)^{37}$S with a ^{36}S beam at 168 MeV ($\sim$4.7 MeV/u) with average intensity of $\sim$0.1 pnA. The beam energy was limited both by the Tandem maximum voltage and the requirement that the fusion barrier with Au was not overcome. The target

was composed of a thin (0.5 mg/cm^2) layer of deuterated polyethylene (C_2D_4) evaporated onto stretched Au backings of 4 and 6 mg/cm^2. The low radiation hardness of the C_2D_4 target put a limitation on the maximum beam intensity that could be delivered.

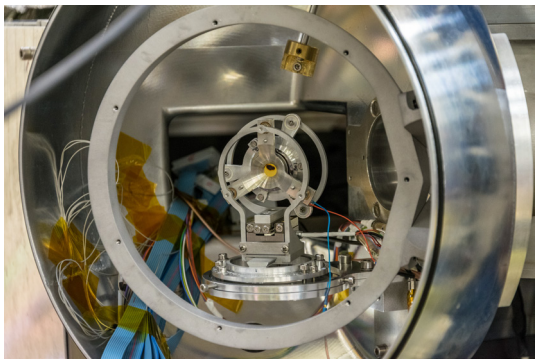

Figure 1. Picture of the plunger device installed in the AGATA scattering chamber for the ^{36}S$(d,p)^{37}$S reaction with a ^{36}S beam at 168 MeV.

The Au backings, on which the target material was evaporated, were used as a degrader for the DSAM, while a 30-mg/cm^2 thick Ta foil, placed at distances from 0.3 to 10 mm from the target, was used as a stopper for beamlike ions. A photograph of the plunger mounted in the AGATA scattering chamber is reported in Fig. 1.
The recoil protons were detected in the SPIDER silicon detector array [12], covering a range of backward angles from 124° to 161°, while the coincident γ rays were detected in AGATA. Figure 2 shows on the top the kinematic line (proton energy as a function of the scattering angle θ) for protons detected in SPIDER in coincidence with AGATA and on the bottom the resulting excitation energy spectrum of the ^{37}S ejectile. This spectrum is reconstructed from momentum conservation in the binary reaction and is an indication of the transfer strength distribution in the final nucleus. The two main structures visible in both plots correspond to the strong transfers to single-particle $p_{3/2}$ and $p_{1/2}$ states at 646 and 2638 keV, respectively. The main $f_{7/2}$ fragment, corresponding to the ground state, is correctly suppressed by the coincidence with γ rays.

We can correlate the excitation energy of ^{37}S with the energy of deexcitation γ rays in a matrix such as the one shown in Fig. 3. The γ-ray energy is Doppler corrected on an event-by-event basis by taking into account the detected proton energy in SPIDER and reconstructing the velocity of the ^{37}S ejectiles, as illustrated in Ref. [13]. Transitions lying on the dashed diagonal are associated to excited states decaying directly to the ground state, the others are instead feeding lower-lying levels. The two transitions with exactly the same energy (1992 keV), from the 1992-keV 3/2$^-$ state and the 2638-keV 1/2$^-$ state, can be distinguished only thanks to this correlation matrix.

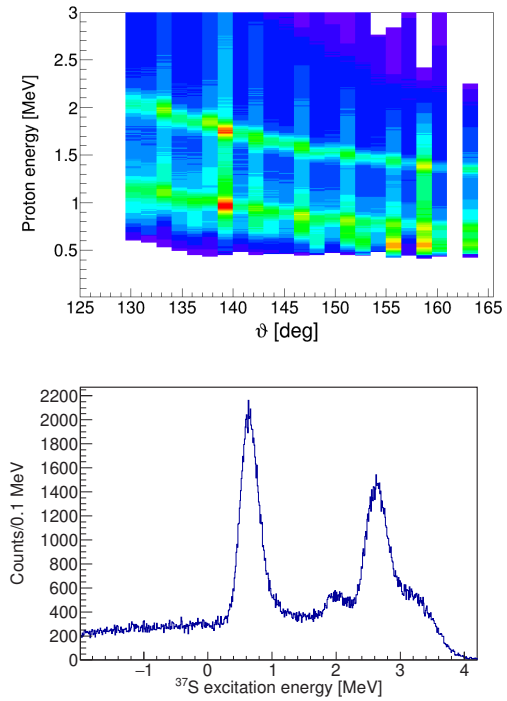

Figure 2. Top: Measured kinematic lines for the d(^{36}S,p)^{37}S reaction at 4.7 MeV/u. Bottom: resulting excitation energy spectrum of ^{37}S. Both spectra have been obtained with a condition on SPIDER and AGATA so the ground-to-ground-state transition is suppressed. The two main structures correspond to the strong transfers to single-particle $p_{3/2}$ and $p_{1/2}$ states at 646 and 2638 keV, respectively.

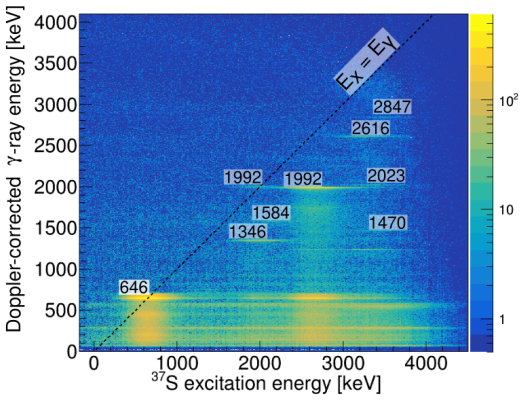

Figure 3. Matrix showing the Doppler-corrected γ-ray energy vs the excitation energy in ^{37}S. The strongest γ-ray transitions are labeled.

It is also very instructive to look at the difference in transfer strength between the direct single-nucleon transfer induced by a light projectile and the one-nucleon transfer in collisions between heavy ions. One may in fact expect different patterns of populations in the final nucleus, since heavy-ion reactions typically involve the transfer of higher angular momenta. Figure 4 shows the levels populated in the present experiment compared to those

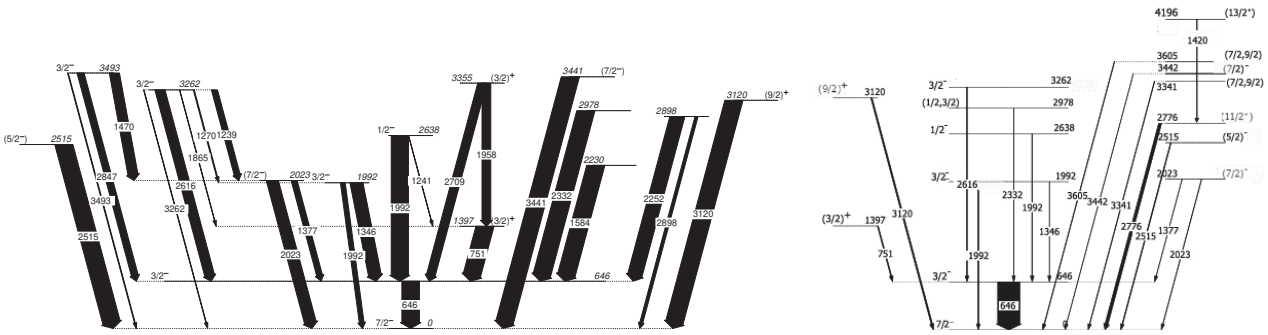

Figure 4. (Left) Levels in ^{37}S populated in the present experiment. (Right) Levels in ^{37}S populated in the MNT reaction ^{36}S+^{208}Pb at 215 MeV (figure taken from Ref. [14]). In both figures, arrows are proportional to the intensity of the transitions.

populated in the multi-nucleon transfer (MNT) reaction ^{36}S+^{208}Pb at 215 MeV, ∼25 % above the Coulomb barrier [14]. One can clearly see how MNT tends to populate yrast states at larger spin with respect to the (d, p) reaction, also because, in reactions between heavy nuclei, it is more likely that the transfer occurs after inelastic excitation of the core. For instance, a significant transfer strength is concentrated in a multiplet of states at ∼3 MeV excitation energy, most likely originating from the coupling of the 2^+ of ^{36}S, which lies at 3.29 MeV and is built on a proton $s^1_{1/2}d^1_{3/2}$ configuration [15], with the unpaired neutron in the $f_{7/2}$. The (d, p) transfer cross section to these states is, obviously, very small.

Therefore, besides being an ideal tool to populate non-yrast low-spin states, from Fig. 2 one can immediately see that, in the direct transfer reaction, selective gates can be set in the excitation energy distribution to select the entry point in the final nucleus. This results in clean γ-ray spectra and the possibility to exclude totally, or at least partially, the feeding coming from higher-lying states.

From the large number of transitions observed in the present experiment, several lifetimes can be determined for the first time in ^{37}S, in some cases placing an upper limit. The only level with a measured lifetime in this nucleus is its first excited state, the $3/2^-$ at 646 keV, whose $B(E2 : 3/2^-_1 \rightarrow 7/2^-_1)$ has a strength of about 3 W. u. and corresponds to a half-life $t_{1/2} \sim 134$ ps [16]. Such lifetime is within the sensitivity of our set-up and can be remeasured with the RDDS technique.

The lifetime analysis is still ongoing and will be subject of a dedicated publication [17].

3 Lifetime measurement of the 2^+_1 state in ^{56}Ni

The $N = Z = 28$ shell closure is the first one arising from the inclusion of a phenomenological spin-orbit force in the nuclear mean-field potential. In a simple shell-model picture, ^{56}Ni, with 28 protons and 28 neutrons, has a doubly closed-shell configuration and is spherical in its ground and first excited states. Theoretical [18] and experimental [19] studies indicate that ^{56}Ni displays instead a rather soft doubly-magic core.

In ^{56}Ni, orbitals above and below the shell closure have the same (negative) parity, allowing the 2^+_1 state to be formed by $1p-1h$ excitations. Therefore, in a pure isospin symmetry picture, the 2^+_1 state should schematically be composed of equal proton and neutron $f^{-1}_{7/2}p^1_{3/2}$ excitations and the corresponding B(E2; $0^+_1 \rightarrow 2^+_1$) should be larger than in neighboring semi-magic isotopes, where neutrons are dominating the wave functions of low-lying excited states.

This is indeed predicted by the shell-model calculations reported in Fig. 5, which calculate a parabolic trend of the B(E2) in Ni isotopes across ^{56}Ni, with a local maximum at the shell closure.

The B(E2; $0^+_1 \rightarrow 2^+_1$) in ^{58}Ni, a stable isotope, is known with high precision from many different techniques. It is well reproduced by the GXPF1A Hamiltonian, which predicts the 2^+_1 level in ^{58}Ni to originate mainly from the coupling of neutrons in the fp shells above $N = 28$. For the unstable ^{56}Ni isotope, the E2 strength measurement is much more challenging. The reduced transition strength B(E2; $0^+_1 \rightarrow 2^+_1$) in ^{56}Ni has been experimentally determined via different methods: relativistic Coulomb excitation [19], proton inelastic scattering [20] and lifetime measurement [21].

As shown in Fig. 5, the experimental results are compatible but present large error bars and, in addition, show some tension with shell-model predictions. The experimental trend of the B(E2) around ^{56}Ni is opposite to the predictions of shell-model calculations, with a minimum at ^{56}Ni instead of the predicted maximum. In addition, the error bar associated with the lifetime measurement (red point) extends down to a B(E2) value which is four times smaller than the one predicted by SM calculations. A smaller B(E2) value in ^{56}Ni compared to ^{58}Ni is at odd not only with shell-model predictions, but also with the intuitive argument on the proton contribution to the wave function due to the isospin symmetry. Tentatively, a B(E2) value in ^{56}Ni smaller than in ^{58}Ni could suggest a large

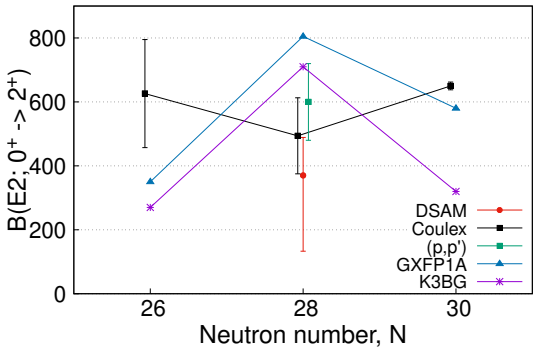

Figure 5. Systematics of the reduced transition probabilities B(E2; $0_1^+ \rightarrow 2_1^+$) in neutron-deficient Ni isotopes. The experimental value for ^{58}Ni (black dot) is based on different measurements and taken from the evaluation of Ref. [22].

isospin breaking, with a mainly neutron wave function of its 2_1^+ state, or a sudden increase of the $N = Z = 28$ shell gap.

Excited states in ^{56}Ni were populated via the two-proton transfer reaction ^{54}Fe(^{16}O,^{14}C)^{56}Ni, with a ^{16}O beam at 80 MeV and average intensity of 2 pnA, delivered by the TANDEM accelerator, impinging on a 0.5-mg/cm^2 thick target of ^{54}Fe.

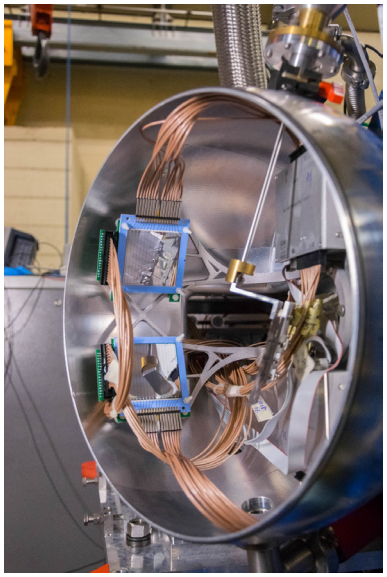

Figure 6. Picture of the experimental set-up for the ^{54}Fe(^{16}O,^{14}C)^{56}Ni reaction with the two OSCAR telescopes installed in the AGATA scattering chamber.

This reaction was shown to populate the 2_1^+ state in ^{56}Ni with a cross section of approximately 100 μb/sr [23], and other low- and medium-spin yrast and non-yrast states with sizable cross sections [24].

The beamlike fragments were detected in the OSCAR detector [25], composed of 2 segmented ΔE-E telescopes (20 μm + 500 μm) placed at forward angles, as shown in Fig. 6. The -2p channel (C) was separated from the Rutherford scattered beam ions and the pure neutron-transfer channels (O) via the ΔE-E technique, as shown in Fig. 7.

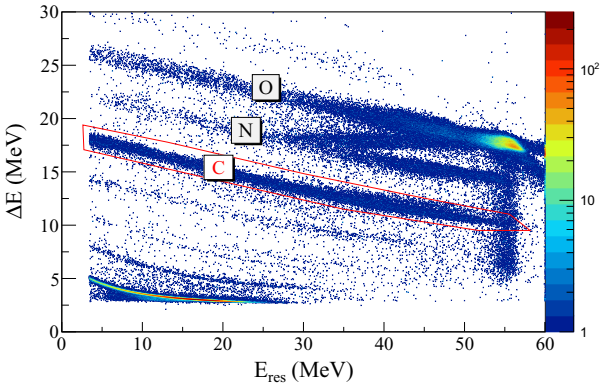

Figure 7. ΔE-E_{res} matrix for a single OSCAR telescope (one single strip and one single pad), showing the clear separation between $Z = 6, 7, 8$ ions.

An important requirement in this measurement is the need to select the direct population of the 2_1^+ state. Any feeding from the long-lived 4_1^+ state 1.23 MeV above, with half-life $t_{1/2} = 1.60(26)$ ps [26], would hamper the measurement of the 2_1^+ half life, expected to be in the range of 40-100 fs. According to Geant4 simulations, the use of the proposed thin target + backing and of segmented Si detectors will allow to reach resolutions in excitation energy of ~ 500 keV, which should be sufficient to set proper gates to exclude feeding from higher-lying states.

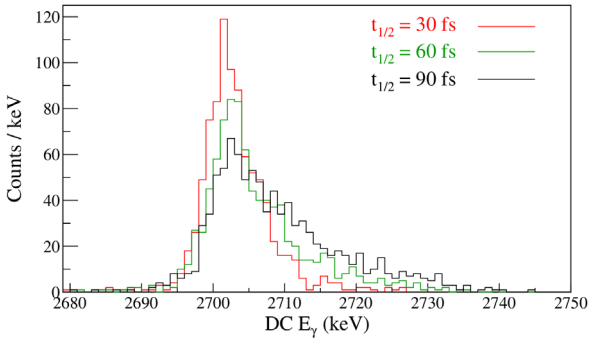

Figure 8. Simulated γ-ray spectra of the $2_1^+ \rightarrow 0_1^+$ transition in ^{56}Ni for different half-lives of the 2_1^+ level, showing the sensitivity of the DSAM in the present experiment.

Considering the short lifetime of the 2_1^+ state (~50 fs) and the low velocity of the ^{56}Ni recoils ($\beta \sim 1\%$), the decay first occurs in the target and eventually in a Nb backing of 0.6 mg/cm^2. The resulting line-shape of the fast transitions of interest can then be compared to Monte Carlo simulations to extract the lifetime of the decaying state. This experimental technique requires the full performance of the AGATA γ-ray tracking array. Figure 8 shows an exam-

ple of simulated line-shapes for different possible lifetimes of the 2_1^+ state, which turn out to be well distinguishable. Analysis is still ongoing to extract the 2_1^+ lifetime and will be discussed in a dedicated publication.

4 Summary and future perspectives

In this contribution, we presented different techniques that have been employed very recently at INFN LNL to measure lifetimes of nuclear excited states in the femtosecond and picosecond range. These states were populated in direct one- and two-nucleon transfer reactions, by detecting the light ejectiles in dedicated set-ups, such as silicon detector arrays and ΔE-E telescopes, and the coincident γ rays in the γ-ray tracking array AGATA. We focused in particular on ^{37}S, populated in a (d, p) reaction in inverse kinematics, and ^{56}Ni, studied via a two-proton transfer in direct kinematics. Lifetimes are determined via the RDDS and DSA methods, according to their different range of applicability.
Such techniques can find application not only with stable beams, but also when, in the near future, re-accelerated radioactive ion beams (RIB) from SPES [27] will be available at LNL with sufficient intensities. The possibility to perform DSAM measurements with RIB has been recently demonstrated [28], coupling AGATA to the array of highly-segmented DSSSD detectors MUGAST and the VAMOS magnetic spectrometer at GANIL [29]. The coupling of high-efficiency and high-resolution compact arrays of silicon detectors, such as GRIT [30], with state-of-the-art γ-ray tracking array as AGATA, will represent one of the most competitive set-ups for this kind of measurements in the years to come.

Acknowledgments

The material presented in this contribution is the result of the cooperative work of many researchers from different institutions and laboratories. The authors would like to acknowledge all the AGATA collaboration.
We are grateful to the LNL accelerator group for providing high-quality beams and the LNL target laboratory for producing highly resistant and uniform targets.

References

[1] S. Akkoyun *et al.* Nuclear Instr. and Methods in Physics Research Section A **668** (2012) 26-58.
[2] A. M. Stefanini *et al.*, Nucl. Phys. A **701** (2002) 217.
[3] S. Szilner *et al.*, Phys. Rev. C **76** (2007) 024604.
[4] J. J. Valiente-Dobón *et al.*, Nucl. Instr. and Meth. A **1049** (2023) 168040.
[5] D. Mengoni *et al.*, Eur. Phys. J. A **59** (2023) 117.
[6] L. Corradi, G. Pollarolo and S. Szilner, J. of Phys. G: Nucl. Part. Phys. **36** (2009) 113101.
[7] E. Caurier, F. Nowacki, and A. Poves, Phys. Rev. C **90** (2014) 014302.
[8] E. K. Warburton, Phys. Rev. C **35** (1987) 2278.
[9] E. K. Warburton, Phys. Rev. C **37** (1988) 754.
[10] C. E. Thorn *et al.*, Phys. Rev. C **30** (1984) 1442.
[11] R. M. Pérez-Vidal *et al.*, Eur. Phys. J. A **59** (2023) 114.
[12] M. Rocchini *et al.*, Nucl. Inst. and Meth. in Phys. Res. A **971** (2020) 164030.
[13] L. Zago, *Mixing between single-particle and intruder configurations towards the N = 20 Island of Inversion: lifetime measurements in ^{37}S*, PhD thesis, Università degli Studi di Padova (2024).
[14] R. Chapman *et al.*, Phys. Rev. C **93** (2016) 044318.
[15] J. J. Valiente-Dobón *et al.*, Phys. Rev. C **98** (2018) 011302(R).
[16] K. L. Wang *et al.*, Phys. Rev. C **94** (2016) 044316.
[17] L. Zago *et al.*, in preparation.
[18] T. Otsuka, M. Honma, and T. Mizusaki, Phys. Rev. Lett. **81** (1998) 1588.
[19] K. L. Yurkewicz *et al.*, Phys. Rev. C **70** (2004) 054319.
[20] G. Kraus *et al.*, Phys. Rev. Lett. **73** (1994) 1773.
[21] N. Schulz *et al.*, Phys. Rev. C **8** (1973) 1779.
[22] B. Pritychenko *et al.*, Nuclear Data Sheets **120** (2014) 112.
[23] F. Pougheon *et al.*, Nucl. Phys. A **193** (1972) 305.
[24] P. R. Christensen *et al.*, Nucl. Phys. A **207** (1973) 33.
[25] D. Dell'Aquila *et al.*, Nucl. Inst. and Meth. in Phys. Res. A **877** (2018) 227.
[26] K. Arnswald *et al.*, Phys. Lett. B **820** (2021) 136592.
[27] https://www.lnl.infn.it/en/spes-2/
[28] I. Zanon *et al.*, Phys. Rev. Lett. **131** (2023) 262501.
[29] M. Assié *et al.*, Nucl. Inst. and Meth. in Phys. Res. A **1014** (2021) 165743.
[30] https://grit.in2p3.fr/